Optimal control of strong-field ionization with time-dependent density-functional theory

Maria Hellgren,[1,2] Esa Räsänen,[3] and E. K. U. Gross[2]

[1]*International School for Advanced Studies, via Bonomea 265, 34136 Trieste, Italy*
[2]*Max-Planck Institute of Microstructure Physics, Weinberg 2, 06120 Halle, Germany*
[3]*Department of Physics, Tampere University of Technology, 33101 Tampere, Finland*

We show that quantum optimal control theory (OCT) and time-dependent density-functional theory (TDDFT) can be combined to provide realistic femtosecond laser pulses for an enhanced ionization yield in few-electron systems. Using a one-dimensional model H_2 molecule as a test case, the optimized laser pulse from the numerically exact scheme is compared to pulses obtained from OCT + TDDFT within the TD exact-exchange (TDEXX) and the TD local-density approximation (TDLDA). We find that the TDDFT pulses produce an ionization yield of up to 50% when applied to the exact system. In comparison, pulses with a single frequency but the same fluence typically reach to yields around 5%–15%, unless the frequency is carefully tuned into a Fano-type resonance that leads to ~30% yield. On the other hand, optimization within the exact system alone leads to yields higher than 80%, demonstrating that correlation effects beyond the TDEXX and TDLDA can give rise to even more efficient ionization mechanisms.

I. INTRODUCTION

Developments in ultrafast science on the electronic time scale have been impressive during the past few years [1]. In particular, manipulation of both intense infrared and weak extreme ultraviolet pulses has led to innovative schemes to measure time delays in the attosecond range [2,3]. It is expected that the ongoing advances will soon open a path into monitoring and controlling real-time electron dynamics.

In addition to measurements on the electronic time scale, subcycle pulse shaping has recently become possible. Wirth *et al*. [4] have generated synthesized laser pulses by combining subcycle transients across the infrared, visible, and ultraviolet regimes. In each regime, the chirp, carrier envelope phase, time delay, and energy (beam size) can be controlled before the final pulse is reconstructed.

The advances mentioned above bring the applications of optimized control schemes, such as quantum optimal control theory [5–7] (OCT), to a new level of practical relevance. In atomic physics, OCT has been previously applied to design laser pulses for, e.g., enhanced [8] and suppressed ionization [9]. For molecular processes the range of applications is significantly larger, covering, e.g., dissociation [10], chemical design [11], and molecular switches [12]. These research lines within OCT among other applications are described in a recent review by Brif *et al*. [7]

On the theoretical side, a single-active-electron approximation is usually employed [13], with the full treatment of many-electron effects being limited to numerical investigations on very small systems. With the aim of studying larger and more complex systems, time-dependent density-functional theory [14,15] (TDDFT) has emerged as a computationally efficient method that can, in principle, exactly deal with the dynamics of the full many-electron system. Within TDDFT the exact time-dependent density is obtained from a fictitious system of noninteracting electrons moving in an effective time-dependent Kohn-Sham (KS) potential. The KS potential is a unique functional of the density which, in practice, must

be approximated. Over the past years different approximation schemes have been developed and tested, showing both promise and future challenges [16–20]. In addition, very recently, the *inverse* problem, i.e., finding the field that drives the many-particle system to a desired outcome, has been formally solved within a combination of OCT and TDDFT [21].

In the present work we take steps in the practical validation of this combination by testing how fields optimized in the TDDFT framework (with different functionals) perform when applied in the numerically *exact* time-dependent Schrödinger equation. This question is of particular relevance from the experimental point of view; namely, when considering a many-electron system beyond the capabilities of a numerically exact treatment, can we design usable laser pulses with TDDFT + OCT to be used in an experiment for an enhanced effect? Our response will be affirmative, but with important reservations, as will be discussed.

We focus on maximizing the total ionization of a model H_2 molecule. First, a target functional in terms of the density is formulated and carefully validated. As our main result we show that the application of OCT in conjunction with TDDFT produces pulses that, when used in the exact system, lead to considerably higher ionization yields than nonoptimized single-frequency fields with the same fluence. However, the lack of correlation effects beyond the simple approximations in the used adiabatic functionals is shown to affect the yield in a negative way. This effect is further exemplified by calculating the ionization yield of H_2 as a function of the (single) photon frequency.

This paper is organized as follows. In Sec. II we introduce the model H_2 system as well as the OCT scheme. In Sec. III we present our main results for the optimization of the ionization yield with different exchange-correlation (XC) functionals in TDDFT and compare with the numerically exact scheme. We also investigate the single-frequency pulses, which further underline the importance of correlation effects. The paper is summarized in Sec. IV.

TH-2013-18

II. SYSTEM AND METHODOLOGY

A. Model Hamiltonian

The H_2 molecule is modeled in terms of a one-dimensional (1D) system with a soft Coulomb interaction between the electrons [8,22]. This model has been shown to capture many qualitative features of the true three-dimensional (3D) molecule, which is enough also for our purposes. The time-independent Hamiltonian of this system is given in Hartree atomic units (a.u.) by

$$H = \sum_{i=1}^{2} \left\{ -\frac{1}{2}\frac{\partial^2}{\partial x_i^2} + V_{\text{ext}}(x_i) \right\} + V_{ee}(x_1, x_2), \quad (1)$$

where the nuclear potential is

$$V_{\text{ext}}(x_i) = -\frac{1}{\sqrt{(x_i - R/2)^2 + a}} - \frac{1}{\sqrt{(x_i + R/2)^2 + a}}, \quad (2)$$

with x_i being the position coordinate of electron i and a being a "softening" parameter for the electron-nucleus interaction; in this work $a = 0.9$. Due to the short duration of the laser pulse (a few femtoseconds) the nuclei are considered to be fixed at their equilibrium separation of $R = 1.5$ a.u. The electron-electron interaction is given by a soft Coulomb interaction according to

$$V_{ee}(x_i, x_j) = \frac{1}{\sqrt{(x_i - x_j)^2 + 1}}, \quad (3)$$

so that here the softening parameter is 1. The exact eigenstates and eigenenergies can be found by the exact diagonalization of H. Applying a time-dependent field implies solving the full time-dependent Schrödinger equation. In this work the system is assumed to be in the ground state $\Psi(t = 0) = \Phi_0$ (a spin singlet) when the laser is switched on. It is easy to see that, numerically, solving a 1D two-electron problem is equivalent to solving a one-electron problem in two dimensions. Such calculations can be carried out using the OCTOPUS code [23], which is our choice for all the results presented in this work.

B. Kohn-Sham system

The TDDFT description of the same system uses the existence of an independent-particle system evolving according to the KS Hamiltonian,

$$H^{\text{KS}} = \sum_{i=1}^{2} \left\{ -\frac{1}{2}\frac{\partial^2}{\partial x_i^2} + V_{\text{KS}}[n](x_i) \right\}, \quad (4)$$

that exactly reproduces the true interacting density,

$$n(x, t) = 2 \int dx' |\Psi(x, x', t)|^2. \quad (5)$$

Due to the Runge-Gross theorem [14] the density uniquely determines all observables as a function of time. The KS potential V_{KS} is normally split into the external V_{ext}, the Hartree $V_H[n]$, and the XC potential $V_{\text{xc}}[n]$. If the external potential is time dependent, V_H and V_{xc} also become time dependent. In this work we have tested two different approximations to V_{xc}: the TD exact-exchange (TDEXX) approximation and the TD local-density approximation (TDLDA). For two electrons the TDEXX approximation is equivalent to the time-dependent

TABLE I. Ionization potentials from the HOMO eigenvalue and excitation energies in TDEXX and TDLDA compared to the exact results (in eV). Also the bare KS-EXX results are presented.

	Exact	TDEXX	KS-EXX	TDLDA
I_p	19.32	19.05	19.05	12.52
ΔE_1	12.25	12.52	10.34	11.70
ΔE_2	15.24	15.51	14.97	

Hartree-Fock approximation, which removes exactly the self-interaction in the Hartree potential. Thus, $V_{\text{x}}(x, t) = -1/2 V_H(x, t) = -1/2 \int dx' V_{ee}(x, x') n(x', t)$. Notice that for a spin singlet as studied in this work there are no additional spin exchange effects. A 1D version of the LDA for soft Coulomb interactions has recently been developed by Helbig *et al.* [18]. Both TDLDA and two-electron TDEXX are adiabatic; i.e., they depend only on the instantaneous density (not on its history).

The equilibrium properties calculated exactly as well as within TDEXX and TDLDA are summarized in Table I. The ionization energy I_p is obtained from the highest occupied molecular orbital (HOMO) of the unperturbed KS system. Excitation energies can be calculated by means of linear response TDDFT [24], in which the exact response function $\chi(\omega)$ (a matrix in x and x') is expressed in terms of a Dyson-like equation containing the Hartree v and an XC kernel $F_{\text{xc}} = \delta V_{\text{xc}}/\delta n$,

$$\chi(\omega) = \chi_s(\omega) + \chi_s(\omega)[v + F_{\text{x}}(\omega)]\chi(\omega). \quad (6)$$

The KS response function χ_s contains the "bare" excitation energies (denoted KS-EXX in Table I). The true excitation energies are obtained from the poles of χ. In TDEXX $F_{\text{x}} = -1/2 V_{ee}(x, x')$, and we find that the two first excitation energies ΔE_1 and ΔE_2 agree well with the exact values. Also the ionization energy is in good agreement with the exact result. TDLDA gives a rather poor ionization energy due to the exponential decay of the LDA-XC potential. The same property leads to only one empty bound state, which, on the other hand, is rather well described.

Even if TDEXX and TDLDA give a reasonable account of the ground and low-lying excited states of the system, it remains to be tested to what extent nonlinear responses can be captured. Previous studies show that, e.g., the adiabatic approximation tends to detune resonances in the nonlinear regime [18]. In the following we will investigate whether it is possible to find a common femtosecond laser pulse that can enhance the ionization yield in *both* the KS system and the exact system.

C. Pulse optimization and the target functional

The laser pulse is treated in the dipole approximation, i.e., $V_{\text{laser}}(x, t) = \varepsilon(t)x$. For the optimization $\varepsilon(t)$ is represented as

$$\varepsilon(t) = \sum_{n=1}^{M} \left[f_n \sqrt{\frac{2}{T}} \cos(\omega_n t) + g_n \sqrt{\frac{2}{T}} \sin(\omega_n t) \right], \quad (7)$$

where the amplitudes $\{f_n, g_n\}$ are varied during the optimization. T is the time duration of the laser pulse; hence $\varepsilon(0) = \varepsilon(T) = 0$. The frequencies $\omega_n = 2\pi n/T$ are

determined on an equidistant grid. In this work $T = 5.3$ fs and the cutoff frequency $\omega_{max} = 9.25$ eV, which fixes the number of frequencies to $M = 12$. The cutoff frequency is chosen to be smaller than the first excitation energy of the H_2 molecule. As we will see this choice still allows for ionization that exploits the excited states. The amplitudes are constrained by keeping the fluence, i.e., the time-integrated intensity, of the laser pulse fixed. This value is determined by the initial pulse given by $\varepsilon(t) = f(t)\cos(\omega_0 t)$, with $\omega_0 = 1.5$ eV and pulse envelope $f(t) = F_0 \cos[\pi/2(t - 3T)/T]$. The amplitude F_0 is chosen to produce a peak intensity of 500 TW/cm^2.

We apply OCT in a so-called direct-optimization scheme presented in detail in Ref. [8]. In practice, we maximize a merit function for a set of parameters of the laser pulse [25] between consecutive time propagations. Expressing the pulse in a proper Fourier basis [8] guarantees that the conditions $\int_0^T dt\, \varepsilon(t) = 0$ and $\varepsilon(0) = \varepsilon(T) = 0$ are satisfied.

In order to maximize the ionization yield we need to formulate a target functional to use in the OCT calculation. In Ref. [8] the ionization target was expressed as an *exclusion* of a set of lowest bound states. Here, in order to apply TDDFT, we need to write the target in terms of the density only. This gives us two choices: (i) we can minimize the density inside radius R, or (ii) we can maximize it outside R at the end of the pulse. In case (i) we minimize the overlap between the density and a Heaviside step function of the form $-\Theta(R - |x|)$, whereas in case (ii) we maximize the overlap between the density and $\Theta(|x| - R)$. In principle, these cases are identical, but due to a finite simulation box and absorbing boundaries we resort to choice (i), apart from the test case described below in this section. We set R to be equal to the box radius (40 a.u.).

The ionization probability P can be determined from the remaining density in the system in the long-time limit, i.e.,

$$P = 1 - \frac{1}{2}\int_{-R}^{R} dx\, n(x, t \to \infty). \qquad (8)$$

In practice we calculate P at $T = 8$ fs, when the density has almost fully converged. As the pulse length is fixed to 5.3 fs, we thus continue the time propagation after the field has been switched off, during which the density continues to evolve in the system.

In Fig. 1 we assess the validity of the density target described above by considering the ionization process of a 1D *single-electron* H_2^+ molecule. The peak intensity of the initial pulse is this time set to 1000 TW/cm^2. Figure 1(a) shows the probability densities of the five lowest eigenstates. The first target operator (target 1) is defined as $1 - \sum_{i=0}^{4} |\Phi_i\rangle\langle\Phi_i|$; i.e., we are attempting to avoid the occupation of the five lowest states. This type of a target for ionization has been validated in previous studies [8]. Alternatively, target 2 is defined from the density by maximizing the overlap with the shaded region in Fig. 1(a) corresponding to $\Theta(|x| - R)$ [case (ii) above]. To enable a direct comparison between the two targets in this example, we use here $R = 15$, which approximately agrees with the spatial extent of the four lowest eigenstates [Fig. 1(a)]. As shown in Fig. 1(b), the results for the decaying number of electrons N in $|x| \leqslant R$ as a function of time, as well as for the optimized pulses (inset), are almost identical for these two targets. In both cases the ionization probability is significantly
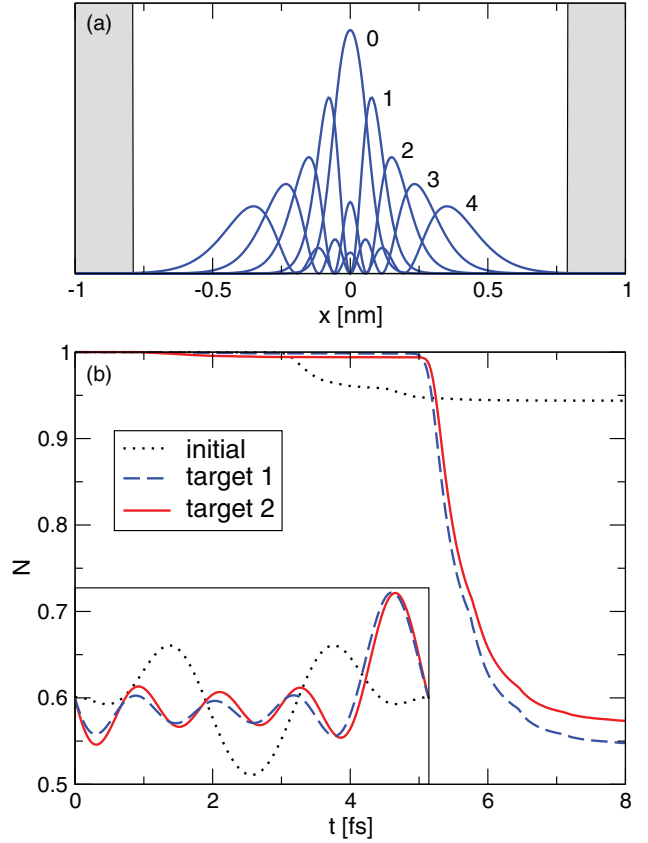

FIG. 1. (Color online) (a) Probability densities of the five lowest eigenstates in a 1D H_2^+ molecule. The first target for ionization is to exclude the occupation of these states (target 1), whereas the alternative target is to maximize the overlap between the density and the shaded region (target 2). (b) Electron number in $|x| \leqslant R$ as a function of time in the presence of the initial pulse (dotted line) and pulses optimized by using target 1 (dashed line) and target 2 (solid line). The pulse profiles are shown in the inset.

increased through optimization. We point out that here the high ionization yield results primarily from the high-intensity peak near the end of the pulse. A detailed discussion on such an OCT process in the tunneling regime can be found in Refs. [8] and [9].

We point out that the obtained pulses are not unique, which is a common feature of all OCT studies. The algorithm finds slightly different pulses depending on the initial condition for the optimization.

III. RESULTS

A. Results for ionization

Now we switch back to the original two-electron H_2 system defined in Sec. II A. Figure 2(a) shows the results obtained from the optimization in the *exact* system. The optimal laser pulse and its Fourier transform are shown in the top left and right panels, respectively. In the bottom panel we show the evolution of the integrated density (normalized to 1) in the system, $N(t) = (1/2)\int_{-R}^{R} dx\, n(x, t)$ (red solid line). Thus, in the long-time limit the ionization probability in Eq. (8) can be expressed as $P = 1 - N(t \to \infty)$. We
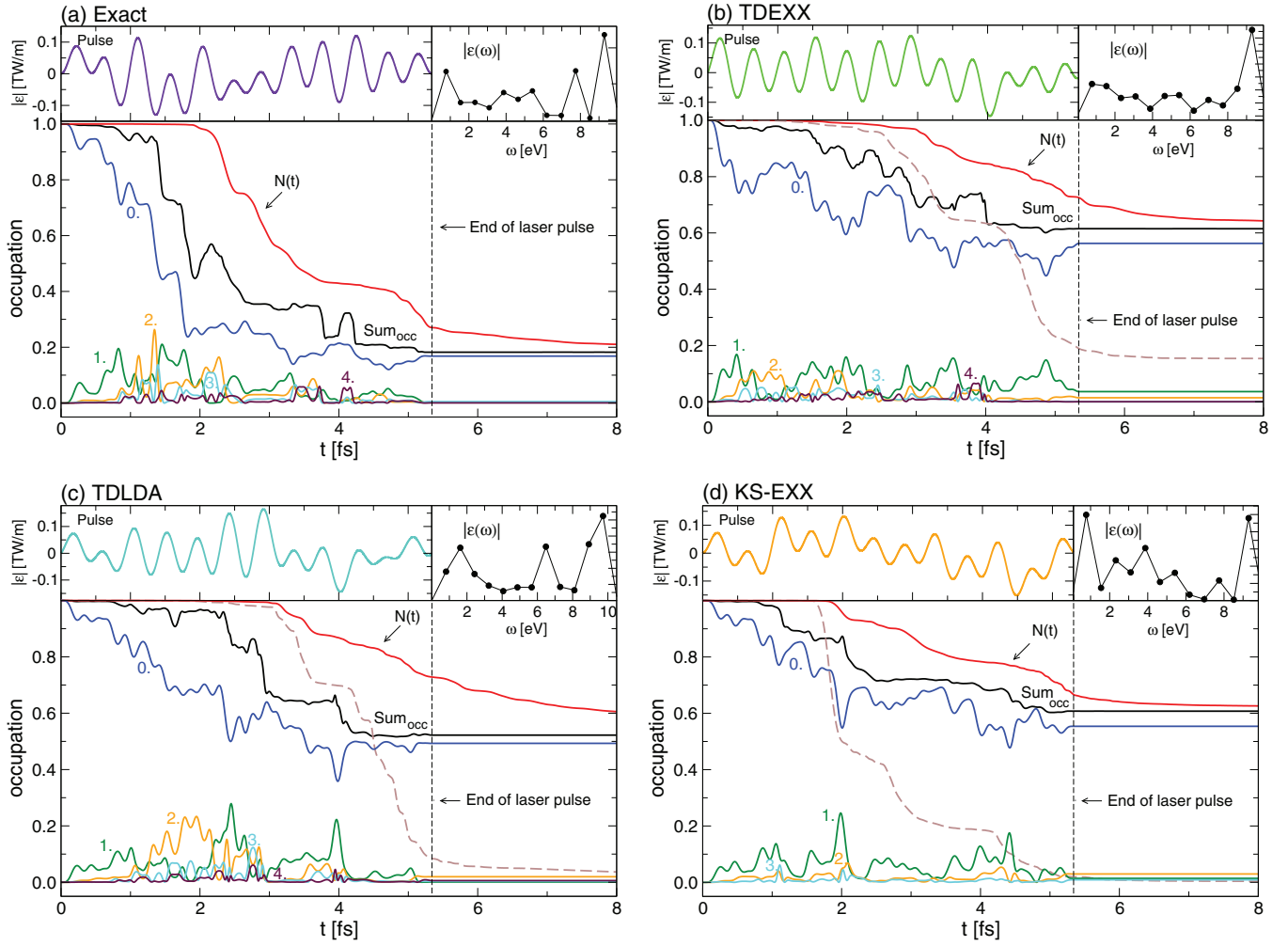
FIG. 2. (Color online) Optimized laser pulses (top left panel), their Fourier transforms (top right panel), and the projections on the excited states as well as the number of particles as a function of time in the exact system (bottom panel) from (a) exact optimization, (b) TDEXX, (c) TDLDA, and (d) KS-EXX. The dashed line in (b)–(d) is the number of particles $N(t)$ in the corresponding KS system under the influence of the same laser pulse.

also plot the projections $|\langle \Psi(t)|\Phi_i \rangle|^2$ $[i = 0, \ldots, 4]$, where $\Psi(t)$ is the time-evolved wave function and Φ_i denotes the ith eigenstate of the unperturbed system. The sum of the projections, corresponding to the total occupation of the four lowest eigenstates, is also shown. It can be expected that in the $t \rightarrow \infty$ limit $N(t)$ approaches the sum of the occupations. This is due to the fact that after the pulse has been switched off, the part of the electron density that is *not* bound in the lowest states eventually propagates *into the absorbing boundaries*. This expectation is confirmed by all the results below.

We see in Fig. 2(a) that already at $t = 2$ fs the probability of an electron being ionized is around 50%. The ionization process is seen to involve the excited states. Mainly, Φ_1 and Φ_2 are exploited, starting with an increased occupation of Φ_1 as the ground state is being deoccupied. Around $t = 1$ fs we find a transfer from Φ_1 to Φ_2, just before the laser reaches its peak intensity, where ionization occurs. A similar effect is repeated thereafter. During the remaining pulse duration, a smooth depopulation of the bound states takes place, and at the end only 20% of the ground state is occupied. Around $t = 8$ fs, the $N(t)$ curve converges to the sum of the projections, and

we find the yield to be 80%. This should be compared with the initial single-frequency pulse giving a yield of less than 10%.

In Fig. 2(b) we show the results obtained by optimizing the laser pulse in the KS system within the TDEXX approximation. By applying this laser pulse to the exact system we find the results of the lower panel. The dashed line in the background is the $N(t)$ curve of the KS density under the influence of the same laser pulse, leading to a final yield of 80% in the KS system. When applied to the exact system, the same laser pulse gives a yield of around 40%. This shows that the densities in the exact and in the TDEXX systems behave quite differently and that the pulse optimized in the TDEXX scheme has only a limited ionization effect on the exact system. Despite its limitations, the KS optimization is seen to produce a better pulse than the initial guess and, as we shall see later, a pulse better than any single-frequency pulse in the allowed frequency range. The projections on the excited states of the exact system show that also with the TDDFT pulse the excited states are involved. The major difference compared to the exact case is that the ground state gets *repopulated* after being depopulated. The transfer to the second excited state or

to the continuum is therefore not complete as in the exact case. This oscillating behavior is seen throughout the pulse duration, and it appears to prevent complete ionization.

Figure 2(c) shows the results from the TDLDA optimization. In this case we are able to find a slightly higher yield of 50% when the pulse is applied to the exact system. We also see that the oscillating behavior is reduced and the second excited state is better exploited than in the TDEXX case.

We have also performed an optimization keeping the KS-EXX potential fixed in time [Fig. 2(d)]. In this way the electrons are treated independently during the time propagation. As expected the optimized pulse now contains less information about the excited states of the system. Only the first one is used when applying this pulse to the exact system. The final yield is, however, still as high as 40%.

In the frequency range between 0 and 9 eV the Keldysh parameter $\gamma = \omega\sqrt{(2I_p)}/E_0$ of the system varies between 1 and 4. This means that we are in a regime where both multiphoton and tunneling ionization are probable. This fact complicates the analysis of the exact mechanism behind the optimal ionization. In addition, the optimized pulses contains a large number of frequencies, and from the Fourier transforms we find no dominant frequency apart from perhaps the highest one. This frequency constitutes, however, a large component in all cases, for high and low yields, suggesting that it is not solely responsible for optimizing the yield. This is indeed confirmed by the single-frequency pulse analysis as we will present in the next section. Finally, we point out that spectral phases are not found to provide us with further information to analyze the optimization procedure.

B. Single-frequency pulses

In order to gain further insight into the ionization processes of H_2 we test the effect of laser pulses containing only a single frequency according to $\varepsilon(t) = f(t)\cos(\omega t)$, where the pulse envelope is given by $f(t) = F_0\cos[\pi/2(t - 3T)/T]$. The amplitude F_0 is chosen to produce a peak intensity of 500 TW/cm^2, and the pulse length is $T = 5.3$ fs. The total propagation time is 8 fs, so that $f(t) = 0$ at $t > T$. The fluence is equal to the one of the OCT processes described above, and the whole frequency range below the cutoff frequency chosen for the optimized laser pulses is scanned. The ionization yield is determined by integrating the density in the simulation box as explained in Sec. II C.

The yield as a function of frequency is plotted in Fig. 3. We only display frequencies between 3.5 and 8.5 eV since outside this range the yield is very close to zero. The exact result (black line with dots) is compared to the TDEXX result (red solid line), the TDLDA (blue line with diamonds), and the KS-EXX (green dashed line). Notice that if the exact time-dependent KS potential were used, the KS yield would be equal to the exact yield since only the density is needed to determine the ionization yield. Distinct peaks are found at certain frequencies. They are strongly emphasized in the noninteracting KS-EXX spectrum, which can be considered our zeroth-order approximation with respect to the Coulomb interaction. This choice of a zeroth-order system leads to the correct description of the ionization energy of the first
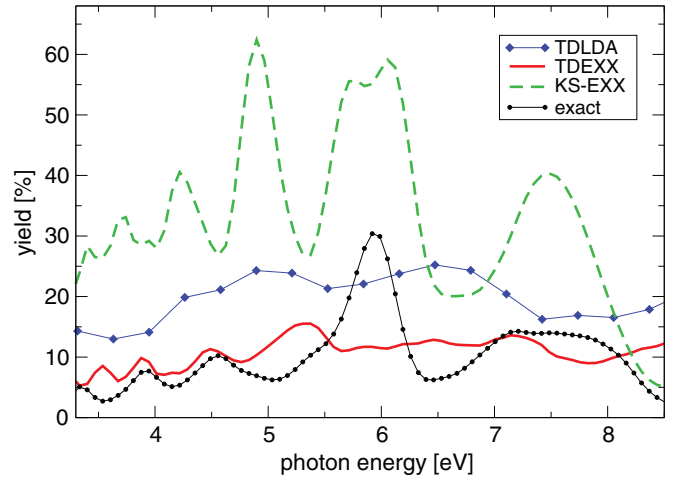

FIG. 3. (Color online) The total ionization yield as a function of laser frequency (photon energy). The pulse duration is 5.3 fs, and the peak intensity is 500 TW/cm^2.

electron but misses the fact that the second electron should be more bound and much harder to ionize. The role of the time-dependent effective potential is to simulate this effect and reduce the yield, here by roughly a factor of 4. This effect is rather well reproduced by the TDEXX. The peaks are also somewhat shifted in the TDEXX and hence in better agreement with the exact result, at least at low frequencies.

At around $\omega = 6$ eV, we find a sharp peak in the exact spectrum that appears to have an asymmetric Fano line shape. Its location is very close to half of the first discrete excitation energy at $\omega = 12.25$ eV. Indeed, using a laser with exactly this frequency causes the yield to peak at 90% in the exact system, showing that this excitation can contribute significantly to optimizing the yield. We note that the other peaks cannot directly be associated with the excitation energies.

In the TDEXX results we find no clear signature of the sharp resonance. The TDLDA curve shows a suppression of the yield, but the effect is less accurate compared to TDEXX. Also here the resonance is missing. The fact that both TDEXX and TDLDA are unable to fully capture resonances related to the excitation energies provides a possible explanation as to why the TDDFT optimizations does not find the optimal mechanism for ionization. In the intensity and frequency range that we have used two photons are required to reach the excited state. The second variation of the TDEXX potential is zero and does therefore not include interaction effects to second order in the external field. This suggests that correlation effects are important to describe the resonance.

The maximum yield we can obtain using a laser pulse with a single-frequency below the first excitation energy and with a peak intensity of 500 TW/cm^2 is around 30%. Thus, even if we were able to locate the resonance, the yield would be still lower than the one obtained in the OCT procedure (within all the tested approximations in TDDFT) that allows for more frequencies. Thus, it is clearly beneficial to use OCT for an enhanced yield as opposed to an optimal single-frequency pulse.

IV. SUMMARY

We have applied quantum optimal control theory in conjunction with time-dependent density-functional theory to examine enhanced ionization of a model H_2 molecule. First, we have validated the use of a density-based target for the maximum ionization in the TDDFT framework. According to our main results, pulse optimization within the (adiabatic) exact-exchange formalism and the local-density approximation provide reasonable pulses for enhanced ionization: when those pulses are applied to the exact system, the yield is considerably increased with respect to the yield of the initial or any single-frequency pulse result. However, we have found that these functionals are unable to capture complicated correlation effects in the system that might lead to an even more efficient ionization mechanism. The presence of these effects becomes clear in the analysis of the exact ionization yield as a function of the pulse frequency, revealing, e.g., a resonance related to the first excited state of the system which is missing in the TDDFT results. In conclusion, TDDFT may be used as the first attempt to optimize strong-field effects in atomic systems, but further work is needed to construct more accurate functionals to account for many-particle phenomena at a deeper level.

[1] F. Krausz and M. Ivanov, Rev. Mod. Phys. **81**, 163 (2009).

[2] M. Schultze, M. Fieß, N. Karpowicz, J. Gagnon, M. Korbman, M. Hofstetter, S. Neppl, A. L. Cavalieri, Y. Komninos, Th. Mercouris, C. A. Nicolaides, R. Pazourek, S. Nagele, J. Feist, J. Burgdörfer, A. M. Azzeer, R. Ernstorfer, R. Kienberger, U. Kleineberg, E. Goulielmakis, F. Krausz, and V. S. Yakovlev, Science **328**, 1658 (2010).

[3] K. Klünder, J. M. Dahlström, M. Gisselbrecht, T. Fordell, M. Swoboda, D. Guénot, P. Johnsson, J. Caillat, J. Mauritsson, A. Maquet, R. Taïeb, and A. L'Huillier, Phys. Rev. Lett. **106**, 143002 (2011).

[4] A. Wirth, M. Th. Hassan, I. Grguras, J. Gagnon, A. Moulet, T. T. Luu, S. Pabst, R. Santra, Z. A. Alahmed, A. M. Azzeer, V. S. Yakovlev, V. Pervak, F. Krausz, and E. Goulielmakis, Science **334**, 195 (2011).

[5] A. P. Peirce, M. A. Dahleh, and H. Rabitz, Phys. Rev. A **37**, 4950 (1988); R. Kosloff, S. A. Rice, P. Gaspard, S. Tersigni, and D. J. Tannor, Chem. Phys. **139**, 201 (1989).

[6] J. Werschnik and E. K. U. Gross, J. Phys. B **40**, R175 (2007).

[7] C. Brif, R. Chakrabarti, and H. Rabitz, New J. Phys. **12**, 075008 (2010).

[8] A. Castro, E. Räsänen, A. Rubio, and E. K. U. Gross, Europhys. Lett. **87**, 53001 (2009).

[9] E. Räsänen and L. B. Madsen, Phys. Rev. A **86**, 033426 (2012).

[10] K. Krieger, A. Castro, and E. K. U. Gross, Chem. Phys. **391**, 50 (2011).

[11] T. Laarmann, I. Shchatsinin, P. Singh, N. Zhavoronkov, M. Gerhards, C. P. Schulz, and I. V. Hertel, J. Chem. Phys. **127**, 201101 (2007).

[12] D. Geppert, L. Seyfarth, and R. de Vivie-Riedle, Appl. Phys. B **79**, 987 (2004).

[13] M. Awasthi, Y. V. Vanne, A. Saenz, A. Castro, and P. Decleva, Phys. Rev. A **77**, 063403 (2008).

[14] E. Runge and E. K. U. Gross, Phys. Rev. Lett. **52**, 997 (1984).

[15] For a review, see C. Ullrich, *Time-Dependent Density-Functional Theory: Concepts and Applications* (Oxford University Press, Oxford, 2012).

[16] M. Mundt and S. Kümmel, Phys. Rev. A **74**, 022511 (2006).

[17] M. Thiele, E. K. U. Gross, and S. Kümmel, Phys. Rev. Lett. **100**, 153004 (2008).

[18] N. Helbig, J. I. Fuks, M. Casula, M. J. Verstraete, M. A. L. Marques, I. V. Tokatly, and A. Rubio, Phys. Rev. A **83**, 032503 (2011).

[19] J. I. Fuks, N. Helbig, I. V. Tokatly, and A. Rubio, Phys. Rev. B **84**, 075107 (2011).

[20] D. Hofmann, T. Körzdörfer, and S. Kümmel, Phys. Rev. Lett. **108**, 146401 (2012).

[21] A. Castro, J. Werschnik, and E. K. U. Gross, Phys. Rev. Lett. **109**, 153603 (2012).

[22] J. Javanainen, J. H. Eberly, and Q. Su, Phys. Rev. A **38**, 3430 (1988).

[23] M. A. L. Marques, A. Castro, G. F. Bertsch, and A. Rubio, Comput. Phys. Commun. **151**, 60 (2003); A. Castro, H. Appel, M. Oliveira, C. A. Rozzi, X. Andrade, F. Lorenzen, M. A. L. Marques, E. K. U. Gross, and A. Rubio, Phys. Status Solidi B **243**, 2465 (2006).

[24] M. Petersilka, U. J. Gossmann, and E. K. U. Gross, Phys. Rev. Lett. **76**, 1212 (1996).

[25] M. J. D. Powell, in *Large-Scale Nonlinear Optimization* (Springer, New York, 2004), pp. 255–297.